Generalized Calculation for Fully Developed Heat and Mass Transfer

WILLIAM N. GILL and MARVIN SCHER

Department of Chemical and Metallurgical Engineering, Syracuse University, Syracuse 10, N. Y.

THE MOST WIDELY applied mass transfer correlation was developed empirically by Chilton and Colburn (2) in 1934 on the basis of heat transfer data existing at the time. The success of this correlation in relating heat and mass transfer coefficients to friction factors led Sherwood (26) to summarize existing methods of correlating mass transfer data and apply von Karman's heat transfer theory to mass transfer. Despite the limitations of this analysis, particularly the assumption of a completely laminar sublayer, the analogy among heat, mass, and momentum transfer was further established. This concept as developed was treated analytically under the fairly restrictive conditions of parallel flow with negligible radial heat and mass transfer, which allows the velocity distribution, the physical properties of the fluid, and therefore the transport processes to be considered unaffected by the transfer rate. Deissler (5) has recently studied analytically the effects of finite heat transfer rates with a corresponding variation of fluid properties across the stream. Finite mass transfer rates have been investigated theoretically for laminar boundary layer flow by Smith (27), Eckert (6-8), Mickley and others (19), Spalding (28), and Merk (17). Experimental work concerning mass transfer with finite interfacial velocities has also been reported (1, 19, 25, 30). However, the ideal case of negligible transfer rates has received considerably more attention both theoretically and experimentally.

Undoubtedly, the recongnition that heat and mass transfer studies provide an effective method for obtaining fundamental information concerning turbulence near solid boundaries stimulated research in this area. The hypothesis necessary to explain the heat and mass transfer results obtained, that turbulence exists up to the wall, is in agreement with the microscopic observations of Fage and Townend (9). In addition, velocity distributions calculated on the basis of this hypothesis are in good agreement with those determined experimentally. The suggestion (3, 13, 14, 23) of investigating this effect at high N_{Pr} and N_{Sc}, where heat and mass transfer are more sensitive to turbulent disturbances than momentum transfer, appears to be valid.

Several semitheoretical heat and mass transfer analyses now exist (5, 13, 15, 16, 22-24) for the case of negligible transfer rates. Each is limited either by approximations which reduce the extensive calculations required to obtain a solution or by proposed functions based on insufficiently detailed experimental data. The work of Martinelli (16), Lyon (15), Seban and Shimazaki (24), and Poppendiek (22) is applicable to low N_{Pr} fluids only since a completely laminar sublayer was assumed. Deissler (5) and Lin, Moulton, and Putman (13) assumed that heat and mass flux were constant across the entire boundary layer and used eddy diffusivity functions for the region very near the wall, which appear to be oversimplified. Reichardt's (23) analysis, which extends his previous work, is similar to this study but the calculations are limited; his final results are given only for tubes at $N_{Re} = 30,000$, and it is felt that the present calculation is based on a more accurate estimate of of the eddy diffusivity near the wall.

· The analysis presented here is not restricted to constant or linear radial fluxes, and the proposed eddy diffusivity function for the region near the wall was determined from concentration distribution data (13) at high N_{Sc} which are very sensitive to the magnitude of ϵ/ν. The calculation applies to fully developed flows, assuming that transfer rates are sufficiently low so that the convective velocity at the wall can be neglected and the physical properties may be assumed constant over the entire radius; the eddy diffusivities of heat, mass, and momentum are assumed equal. Some experimental work concerning the ratio of eddy diffusivities exists (12, 21) and is discussed by Hinze (11) among others. Deissler (4), on the basis of an approximate analysis, also obtained an empirical expression for this ratio. However, until more precise measurements, including temperature fluctuations, are made, it does not seem advisable to include its effect, since results are conflicting (11). This assumption affects the results significantly only at low N_{Pr}, where existing experimental data vary considerably within and between investigations. To obtain an essentially exact solution within the assumptions made, integrations were performed numercially by means of an IBM 650 digital computer.

The following discussion pertains to mass transfer; however, if it is assumed that the eddy properties for heat and mass transfer are the same, the results are applicable to heat transfer as well. Therefore, N_{Nu} and N_{Sh} as well as N_{Pr} and N_{Sc} are used interchangeably, as are dimensionless flux and θ distributions.

The shear stress and mass flux equations may be written in dimensionless form as

$$\mathrm{T}/\mathrm{T}_0 = \left(\frac{\mu}{\mu_0} + \frac{\rho}{\rho_0} \frac{\epsilon}{\mu_0/\rho_0} \right) \frac{d\beta}{d(y/b)} \bigg/ \left[\frac{d\beta}{d(y/b)} \right]_0 \quad (1)$$

$$N/N_0 = \left[\left(\frac{D}{D_0} \right) + \left(\frac{\epsilon_d}{\epsilon} \right) \left(\frac{\epsilon}{\nu_0} \right) \left(\frac{\nu_0}{D_0} \right) \right]$$

$$\left(\frac{d\theta}{d(y/b)} \right) \bigg/ \left[\frac{d\theta}{d(y/b)} \right]_0 \quad (2)$$

where

$\beta = \bar{u}/u_{max}$

$\theta = \dfrac{C - C_0}{C_c - C_0}$

$y = $ distance from wall

$b = r_0$ for tubes and half the channel width for flat plates

Equation 2 may be dealt with directly, but at high N_{Sc} the unaccomplished concentration change, θ, approaches unity at a very short distance from the wall. Therefore, as suggested by Reichardt (23), the concentration distribution can be more accurately determined by integrating over β rather than y/b. This is easily accomplished using

$$\frac{d\theta}{d(y/b)} = \frac{d\theta}{d\beta} \frac{d\beta}{d(y/b)} \quad (3)$$

Then Equations 1 to 3 may be combined to obtain

$$\frac{d\theta}{d\beta} = \left(\frac{d\theta}{d\beta}\right)_0 \frac{N/N_0}{T/T_0} \frac{1 + \epsilon/\nu}{1 + N_{Sc} \frac{\epsilon_d}{\epsilon} \frac{\epsilon}{\nu}} \qquad (4)$$

for the case of constant physical properties across the channel. The stress ratio is known to be linear for fully developed flows with negligible convective velocities at the wall, but the mass flux ratio remains to be determined. By an over-all mass balance,

$$N_0 = bU \frac{\partial C_b}{\partial x} \qquad (5)$$

the continuity equation for parallel flow between flat plates may be written

$$\frac{\partial (N/N_0)}{\partial y} = -\frac{1}{b}\left(\frac{\bar{u}}{U}\right) \frac{\partial C}{\partial x} \Big/ \frac{\partial C_b}{\partial x} \qquad (6)$$

and for a fully developed concentration field bounded by a constant wall concentration, which for mass transfer calculations is generally more appropriate than constant mass flux,

$$\frac{\partial}{\partial x}\left(\frac{C - C_0}{C_b - C_0}\right) = 0 \qquad (7)$$

Using the definition of the bulk mean concentration, differentiating with respect to x, substituting into Equation 6, and combining the result with Equation 7, there is obtained after rearranging and integrating

$$\frac{N}{N_0} = 1 - \frac{\int_0^{y/b} \beta\theta d(y/b)}{\int_0^1 \beta\theta d(y/b)} \qquad (8)$$

Combining Equation 8 with Equation 4 and introducing the linear stress relationship there results after integration:

$$\theta = \left(\frac{d\theta}{d\beta}\right)_0 \int_0^\beta \left[\frac{1 + \epsilon/\nu}{1 + (N_{Sc})\left(\frac{\epsilon_d}{\epsilon}\right)\frac{\epsilon}{\nu}}\right]$$
$$\left[\frac{1 - \frac{\int_0^{y/b} \beta\theta d(y/b)}{\int_0^1 \beta\theta d(y/b)}}{1 - y/b}\right] d\beta \qquad (9)$$

Equation 9 may be solved by assuming a concentration distribution, θ, and iterating until the assumed and calculated distributions are identical. A reasonable first approximation is obtained by calculating the concentration distribution using Equation 9 and assuming

$$\frac{N/N_0}{T/T_0} = 1$$

For low N_{Sc} Equations 2 and 8 may be combined directly to obtain

$$\theta = \left[\frac{d\theta}{d(y/b)}\right]_0 \int_0^{y/b} \left[\frac{1 + \frac{\int_0^{y/b}\theta d(y/b)}{\int_0^1 \beta\theta d(y/b)}}{1 + \left(N_{Sc}\frac{\epsilon_d}{\epsilon}\right)\frac{\epsilon}{\nu}}\right] d(y/b) \qquad (10)$$

which is solved by the same procedure as Equation 9.

The discussion through Equation 4 is general and applies to either tubes or plates. To solve the case for circular tubes, it is necessary only to develop an appropriate mass flux distribution. By an argument similar to that just given it is easily shown that for parallel flow in tubes

$$(1 - y/r_0)(N/N_0) = 1 - \frac{\int_0^{y/r_0}[1 - (y/r_0)]\beta\theta d(y/r_0)}{\int_0^1 [1 - (y/r_0)]\beta\theta d(y/r_0)} \qquad (11)$$

This result, combined with Equation 4, gives the desired concentration after integration. Furthermore, the heat transfer equations are identical in form and the results obtained may be considered applicable to heat transfer as well as mass transfer for both flat plates and tubes. The coefficients $\left(\frac{d\theta}{d\beta}\right)_0$ and $\left[\frac{d\theta}{d(y/b)_0}\right]$ may be evaluated from the boundary conditions

$$\theta = 1 \text{ at } \beta = y/b = 1$$

It was predetermined that the solution would be considered exact when the coefficients remained constant in the fourth place upon successive iterations.

Inspection of Equations 9 and 10 indicates that the quantities, ϵ_d/ϵ, ϵ/ν, and the velocity distribution must be known as a function of position if a rigorous calculation is to be made. Since the velocity distribution is determined once ϵ/ν is specified, ϵ/ν will be considered first. Instead of determining ϵ/ν in the vicinity of the wall from velocity distribution data which are relatively insensitive to its magnitude near a solid boundary, the concentration distribution data of Lin (13) were used for this purpose. Lin's interferometer measurements extend to $y^+ = 0.5$, which is much closer to the wall than any other concentration measurements, and appear to be sufficiently accurate to yield a good estimate of the eddy diffusivity in this region. These data are probably more accurate than can be obtained from velocity distribution measurements with present equipment, since at high N_{Sc} concentration gradients very near the wall are much larger than corresponding velocity gradients.

After careful examination of these data, it was found that the eddy diffusivity functions proposed by Lin (13), Deissler (5), and Reichardt (23) were at variance with Lin's experimental concentration distributions and therefore a new function was determined which satisfied these data more exactly. This required extensive reiterative calculations to

Table I. θ_m as a Function of N_{Re} and N_{Sc} for Flow between Smooth Infinite Parallel Plates

$N_{Pr} = N_{Sc}$	N_{Re}									
	5000	10,000	11,000[a]	22,000[a]	25,000	50,000	55,000[a]	100,000	110,000[a]	220,000[a]
0				0.699						
0.001		0.691	0.690	0.684	0.685				0.682	0.683
0.01	0.710	0.698	0.697	0.694	0.696	0.699	0.700	0.711		0.727
0.10		0.745			0.757			0.791		
0.73			0.846	0.857			0.871		0.880	0.889
1.00			0.864	0.874	0.876		0.886		0.893	0.900
5.00			0.937	0.942			0.949		0.949	0.951
10.00			0.960	0.962	0.962		0.966		0.966	0.968
50.00			0.968	0.987			0.989		0.989	0.989
100.00			0.992	0.992			0.993		0.993	0.994
500.00				0.997						
900.00			0.999	0.998			0.999		0.999	0.999
1000.00				1.000						
3000.00	1.000	1.000	1.000	1.000	1.000	1.000	1.000	1.000	1.000	1.000

[a]Values calculated initially based on Equation 12 for region, $0 \leqq y^- \leqq 8$.

obtain the experimental values of ϵ/ν with the single assumption that the ratio ϵ_d/ϵ is equal to unity, $N_{Sc} = 900$, which, according to both Deissler (5) and Reichardt (23), is an excellent assumption at the very high N_{Sc} involved. First a velocity distribution was assumed, and from this and the observed concentration distribution, ϵ/ν was calculated using Equation 4, which in turn yielded a new velocity distribution. This procedure was repeated until ϵ/ν remained unchanged. Since there is some scatter in the Lin data, an ϵ/ν distribution was used that best satisfied all runs made. This distribution is given by

$$\epsilon/\nu = 8.15 \times 10^{-4}(u^+y^+)^{3/2} - 1.159 \ 10^{-4}(u^+y^+)^{5/2} + 7.836 \times 10^{-6}$$

$$(u^+y^+)^{7/2} - 1.645 \times 10^{-7}(u^+y^+)^{9/2} + 1.114 \times 10^{-9}(u^+y^+)^{11/2} \quad (12)$$

for $y^+ \leqq 8$. Initially this polynominal was used for the region $y^+ \leqq 8$ and the Deissler eddy diffusivity function

$$\epsilon/\nu = (0.124)^2 u^+y^+(1 - e^{-0.124^2 u^+y^+}) \quad (13)$$

was used for the region $8 \leqq y^+ \leqq 26$. The velocity distribution over the entire region near the wall, $y^+ \leqq 26$, was determined by combining Equations 12 and 03 with

$$u^+ = \int_0^{y^+} \left(\frac{1}{1 + \epsilon/\nu}\right) dy^+ \quad (14)$$

Sherwood and Nusselt numbers were calculated for both tubes and flat plates on this basis; however, the results were low for N_{Pr} and N_{Sc} between 50 and 500. Good agreement with experiment is obtained in this range if Equation 12 is used for $y^+ \leqq 2$, and Equation 13 for $2 \leqq y^+ \leqq 26$. The reported results correspond to this choice for the eddy diffusivity function, but some results using the initial choice are given in Tables I to IV for comparison.

Although a number of experimental investigations of the velocity distributions between flat plates have been carried out, the results differ to some extent. Opfell and Sage (20) have discussed these studies and concluded that Deissler's (3) distribution for tubes

$$u^+ = 3.8 + 2.78 \ln y^+ \quad (15)$$

is probably most suitable for the turbulent core. When used for flat plates, this distribution presents some difficulties that affect the heat results at low N_{Pr}, where the turbulent core assumes more significance. It is easily shown that for flat plates Equation 15 does not yield the maximum velocity at the center of the channel, and this conflicts with the assumption of symmetrical flow. Therefore a symmetry correction on the order of 3% was applied to Equation 15 for each N_{Re} used. This correction was compensated for in the final calculation of N_{Nu}. For tubes, Equations 12 and

Table II. θ_m Function of N_{Re} and N_{Sc} for Circular Tubes

N_{Sc}	N_{Re} 10,000	25,000	50,000	100,000
0	0.480			0.478
0.001	0.485		0.488	0.491
0.01	0.499	0.506		0.549
0.10	0.596	0.630	0.660	0.691
0.73	0.764			0.817
1.00	0.791	0.811	0.824	0.836
5.00	0.905		0.917	0.920
10.00	0.935	0.940		0.944
20.00	0.960			
50.00	0.978		0.982	0.982
100.00	0.987	0.989		0.990
500.00	0.996			
900.00		0.998	0.998	0.999
1,000.00	0.998			0.999
3,000.00	0.999	1.000	1.000	1.000
6,000.00	1.000			
30,000.00	1.000			

Table III. Nusselt Numbers for Parallel Flow in Smooth Circular Tubes

N_{Sc}	N_{Re} 10,000	10,000[a]	25,000	50,000	100,000	100,000[a]
0	4.53				5.0	
0.001	4.57			5.38	5.69	
0.01	5.33		6.73		11.00	
0.1	10.65		18.48	28.54	44.68	
0.73	29.21				171.0	
1.00	34.15		70.86	121.7	207.6	
5.00	70.97	69.15			496.7	487.3
10.00	93.09		208.7		676.2	
50.00	162.2	145.32			1240.0	1108.0
100.00	203.0	178.5	465.0	855.5	1559.0	1374.0
500.00	342.5	307.6			2665.0	
900.00			957.6			2670.0
1000.00	431.8				3351.0	
3000.00	628.4	603.7	1444.0	2666.0	4880.0	4686.0

[a] Values calculated initially based on Equation 12 for region $0 \leqq y^+ \leqq 8$.

13 combined with Equation 14 for the region close to the wall and Equation 15 for the turbulent core were used without correction except for the lowest N_{Re}, where 3% correction to Equation 15 was required.

It can readily be shown that N_{Sh} may be obtained for tubes by

$$N_{Sh} = \frac{kd}{D} = 2\left[\frac{d\theta}{d(y/b)}\right]_0 = \frac{f}{2}\frac{U}{u_{max}}N_{Re}\left[\frac{d\theta}{d\beta}\right]_0 \quad (16)$$

and for plates by

$$N_{Sh} = \frac{kd_e}{D} = 4\left[\frac{d\theta}{d(y/b)}\right]_0 = \frac{f}{2}\frac{U}{u_{max}}N_{Re}\left[\frac{d\theta}{d\beta}\right]_0 \quad (17)$$

where

$$d_e = 4b$$
$$(N_{Re})_{tubes} = 2b\rho U/\mu$$
$$(N_{Re})_{plates} = 4b\rho U/\mu$$

Table IV. Nusselt Numbers for Parallel Flow between Smooth Infinite Parallel Plates

$N_{Pr} = N_{Sc}$	N_{Re} 5000	10,000	25,000	50,000	100,000
0.001		7.75	8.42	8.81	9.38
0.01	6.71	8.40	9.89	11.60	14.14
0.1		12.78	21.09	31.20	48.03
1.0			71.99		
10			204.9		
100			452.6		
1000			963.1		
3000	313.5	606.5	1402		4756

These N_{Sh} are, however, based on the concentration difference between the wall and the center of the channel and must be transformed to those related to the bulk mean concentration using

$$(N_{Sh})_b = \frac{kd_e}{D} \quad \frac{N_{Sh}^{U/u_{max}}}{\int_0^1 \theta\beta d(y/b)} \quad (18)$$

for flat plates and

$$(N_{Sh})_b = \frac{N_{Sh} \ U/u_{max}}{2\int_0^1 (1 - y/r_0) \ \beta\theta \ (y/r_0)} \quad (19)$$

for tubes. The N_{Sh} values reported subsequently were

determined from these expressions where k_b is defined by

$$k_b = \frac{N_0}{C_0 - C_b} \qquad (20)$$

The term $U/u_{\max}$ in Equations 18 and 19 was determined conventionally by

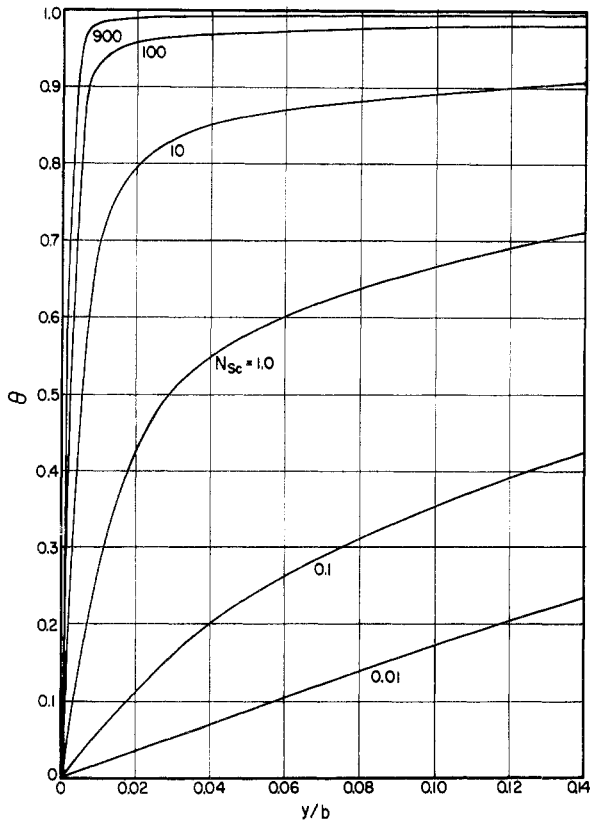$$U/u_{\max} = \int_0^1 \beta d(y/b) \qquad (21)$$

Figure 1. Temperature or concentration distributions for smooth circular tubes at various N_{Pr} or N_{Sc} for $N_{Re} = 25,000$
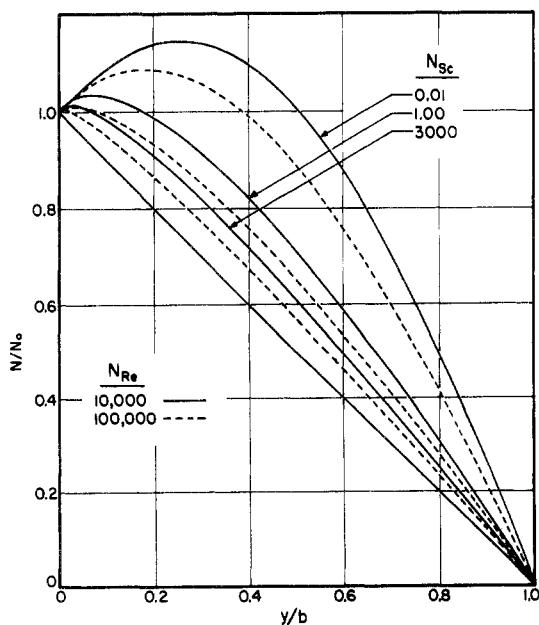
Figure 2. Mass flux distributions for flow in smooth circular tubes

and

$$U/u_{\max} = 2 \int_0^1 (1 - y/r_0)\, \beta d(y/r_0) \qquad (22)$$

for plates and tubes, respectively.

Also of interest are the bulk mean values of θ defined by

$$\theta_b = u_{\max}/U \int_0^1 \beta \theta d(y/b) \qquad (23)$$

for plates, and

$$\theta_b = 2u_{\max}/U \int_0^1 (1 - y/r_0)\, \beta \theta d(y/b) \qquad (24)$$

for tubes. Results of these integrations are given in Table I to IV.

ANALYTICAL RESULTS FOR FLOW IN SMOOTH CIRCULAR TUBES

The concentration distribution for circular tubes is given by

$$\theta = \left(\frac{d\theta}{d\beta}\right)_0 \int_0^\beta \left[\frac{1 + \epsilon/\nu}{1 + N_{Sc}\, \frac{\epsilon_d}{\epsilon}\, \frac{\epsilon}{\nu}} \right]$$

$$\left[1 - \frac{\frac{\int_0^{y^{ib}}(1 - y/r_0)\beta\theta d(y/r_0)}{\int_0^1(1 - y/r_0)\beta\theta d(y/r_r)}}{(1 - y/r_0)^2} \right] d\beta \qquad (25)$$

Representative solutions to this equation are shown in Figure 1. As with flat plates, the diffusion boundary layer
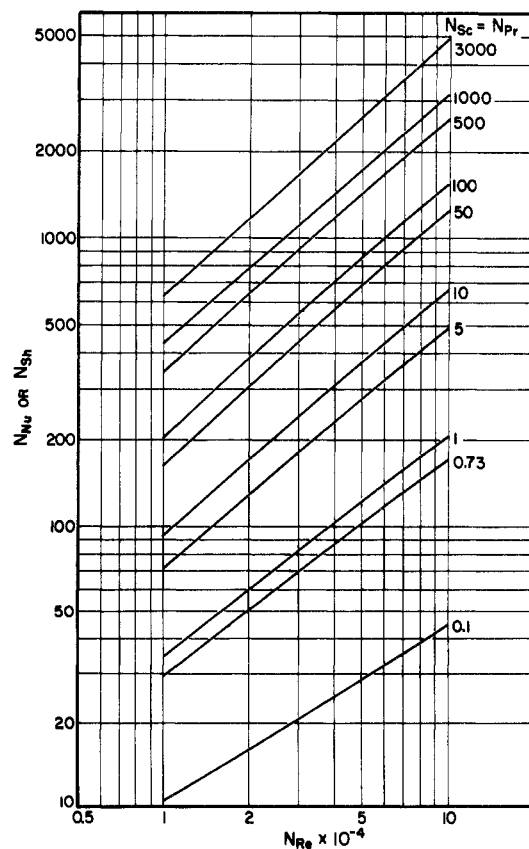
Figure 3. Nusselt numbers for heat or mass transfer in smooth circular tubes as a function of N_{Re} with N_{Pr} or N_{Sc} as parameter

350

moves progressively closer to the wall as N_{Pr} or N_{Sc} and N_{Re} increase.

The representative mass and heat flux distributions shown in Figure 2 indicate a significant difference between the propagation of heat or mass in tubes and flat channels. For tubes the flux at some distance from the wall exceeds that at the wall by as much as 15% for very low N_{Pr}. In general, the heat or mass flux distribution for circular tubes differs considerably more from the linear momentum flux distribution than for flat plates. Consequently, the effect of the nonlinear flux distribution on N_{Nu} is more pronounced than for flat plates, particularly at low N_{Pr}.

N_{Sh} values for circular tubes are presented in Figures 3 to 6. Comparison of the results in Figure 3 with those obtained by Deissler (5) indicates reasonably good agreement except in the region of very high N_{Sc}, where this analysis gives higher values. For example, at $N_{Sc} = 3000$, this analysis for circular tubes gives N_{Nu} values approximately 19% higher at $N_{Re} = 10,000$ and 30% higher at $N_{Re} = 100,000$. In the region of N_{Sc} approximately equal to 1 or less, this analysis gives values below those of Deissler; this agrees with experimentally determined values. Comparison of both these analyses with the Chilton-Colburn empirical correlation indicates agreement in the neighborhood of one, but the analytical results are higher at higher N_{Sc}. It is seen in Figure 4 that for N_{Pr} or N_{Sc} on the order of 10 the results for circular tubes and flat plates are essentially coincident. In contrast, at very low N_{Pr} the results for tubes are considerably below those for infinite parallel plates. This result is to be expected, since in the high N_{Pr} or N_{Sc} region, the heat or mass flux distributions, which differ considerably for the two configurations over the complete channel radius, approach unity immediately adjacent to the wall, where

transfer effects are most pronounced. At low Prandtl or Schmidt numbers the diffusion boundary layer becomes thicker and the effect of the flux distributions extends deeper into the channel. Consequently at very low N_{Pr} the N_{Nu} values for tubes are significantly below the flat plate values as seen in Figure 5.

It is of particular interest that the limiting value of N_{Nu} is 4.53 for tubes at $N_{Re} = 10,000$ and $N_{Pr} = 0$. This limiting value is approximately 10% lower than these obtained previously (23, 24) and is in better agreement with experimental liquid metal heat transfer data, which are usually lower than predicted values. Deissler (4) analyzed low N_{Pr} heat transfer for constant heat flux in tubes and accounted for the variation of q/q_0 with radial distance. His results are higher because of the different boundary condition used.

Recently an experimental heat transfer study of high N_{Pr} fluids has been reported by Friend and Metzner (10). The results were correlated using a relationship proposed by Reichardt (23) and are compared with the present analysis and the Chilton-Colburn correlation in Figure 6. Friend and Metzner's results are higher in the high N_{Pr} region than those obtained analytically. These investigators also compared their correlation with mass transfer data. In particular Linton and Sherwood's (14) data were reported as substantiating and extending the applicability of their correlation. These experimental data have been reported to agree with three correlations (5, 10, 13) which in the N_{Sc} region investigated differ considerably from one another. This is undoubtedly due to the scatter of the data, and mean values at a given N_{Re} are usually used. To eliminate this objection an equation which agrees well with the present analytical results in the N_{Sc} range from 1000 to 3000 was developed in the form,

$$N_{Sh} = CN_{Re}{}^{a}N_{Sc}{}^{b}$$

and is given by

$$(k/V)N_{Sc}{}^{0.63} = 0.0102\,N_{Re}{}^{-0.122} \qquad (26)$$

This equation is a good approximation in this region, since essentially straight lines are obtained from log-log plots of N_{Nu} vs. either N_{Re} or N_{Sc}, as seen in Figures 3 and 4. Equation 26 is compared with all the turbulent flow results of Linton and Sherwood in Figure 7. This relation agrees exceedingly well with the data obtained in 5.23-cm. tubes; however, the results for the 1.9-cm. tubes deviate in both directions from the predicted line. It is probable that the 1.9-cm. benzoic acid tubes were characterized by roughness ratio significantly different from zero, which would explain their high values.

The low values for the 1.9-cm. tubes are more difficult to explain. It might be argued that these results represented smooth surface conditions; however, the heat transfer correlation obtained by Friend and Metzner was presumably obtained under smooth wall conditions and predicts
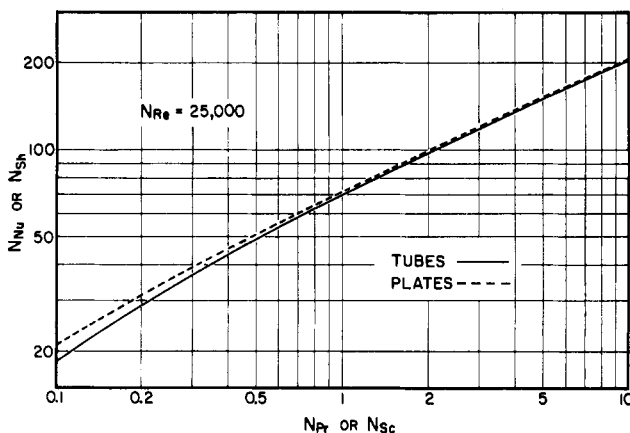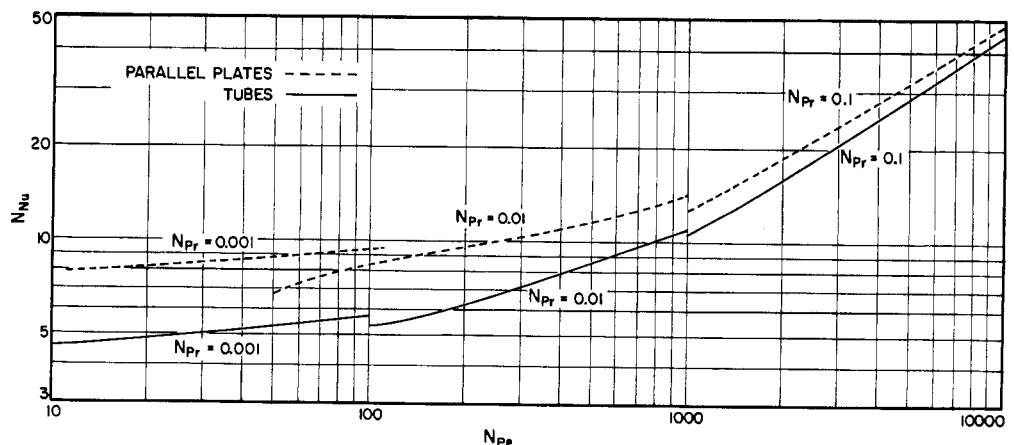

Figure 4. N_{Sh} or N_{Nu} values for smooth circular tubes and infinite parallel plates at $N_{Re} = 25,000$

Figure 5. Nusselt numbers for heat transfer as a function of N_{Pe} at low N_{Pr}
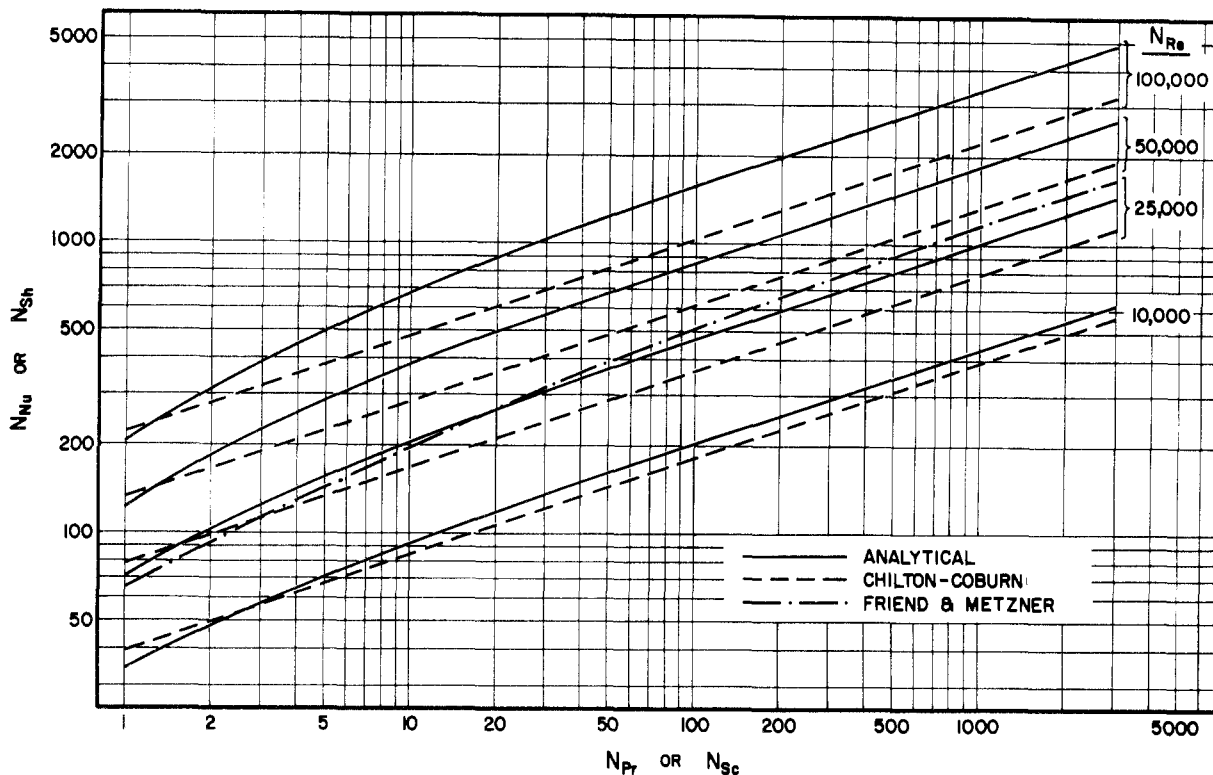
Figure 6. Comparison of analytical solutions for smooth circular tubes with Chilton-Colburn and Friend-Metzner correlations
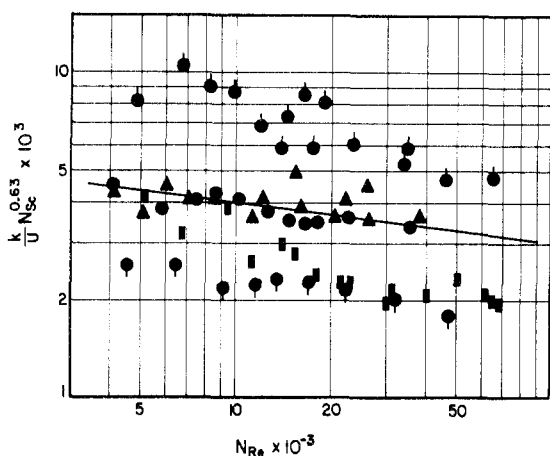

Figure 7. Correlation of Linton and Sherwood Data
(14) for N_{Sc} from 900 to 3500

▲ BENZOIC ACID – 5.23 CM. I.D. TUBE
● CINNAMIC ACID – 5.23 CM. I.D. TUBE
◖ BENZOIC ACID – 1.9 CM. I.D. TUBE
◗ 2-NAPHTHOL – 1.9 CM. I.D. TUBE
▮ CINNAMIC ACID – 1.9 CM. I.D. TUBE

$$\frac{k}{U} N_{Sc}^{0.63} = 0.0122 \, N_{Re}^{-0.122}$$

values higher than Equation 26. It is known that a finite interfacial velocity caused by mass transfer and directed into the stream tends to depress the transfer coefficients; however, this effect was apparently small in the Linton and Sherwood experiments and therefore it does not seem realistic to attribute the low values to this effect.

Although no well-established explanation of the scatter of these data can be offered, further insight into turbulence adjacent to solid boundaries may be obtained from heat and mass transfer investigations at high N_{Pr} and N_{Sc} only if roughness effects are evaluated from friction factor measurements on the same system and, in the case of mass

transfer, if the effects of mass transfer rates are considered. Roughness effects are particularly important at high N_{Pr} or N_{Sc}, since they markedly influence eddy properties near the wall, which is the important region in this case. An interesting study of roughness effects on velocity distributions and friction factors has been made by Van Driest (29), wherein the roughness ratio is considered to counteract the dampening effect of the wall on the eddy diffusivity. This approach can be easily extended to determine roughness effects on forced convection heat and mass transfer.

After this investigation was completed, additional experimental data for benzoic acid, cinnamic acid, and aspirin in water were reported by Meyerink and Friedlander (18). These data are much more consistent than those of Linton and Sherwood. The benzoic and cinnamic acid data were most extensive, and include 37 average values, each of which includes several measurements in the fully developed region. The authors gave least square lines for these and 14 similar measurements for aspirin. These data are compared with Equation 26 in Figure 8. The agreement is considered very good, particularly for the benzoic and cinnamic acid data, where the agreement is well within experimental error. None of the previously mentioned analyses agree as well. Friend and Metzner's (10) and Reichardt's (23) results are consistently higher and Deissler's (5) are consistently lower than both sets of data.

ANALYTICAL RESULTS FOR FLOW BETWEEN INFINITE PARALLEL PLATES

Representative solutions to Equations 9 and 10 are presented in Figure 9. The diffusion boundary layer moves progressively closer to the wall as N_{Sc} or N_{Pr} increases. A similar effect is obtained for increasing N_{Re}.

Representative mass flux distributions, N/N_0, are shown in Figure 10 as a function of N_{Sc} and N_{Re}. As N_{Sc} increases, the flux approaches linearity in y/b and conversely deviates more significantly from linearity for small values of N_{Sc} or N_{Pr}. The deviations from linearity increase rapidly at low
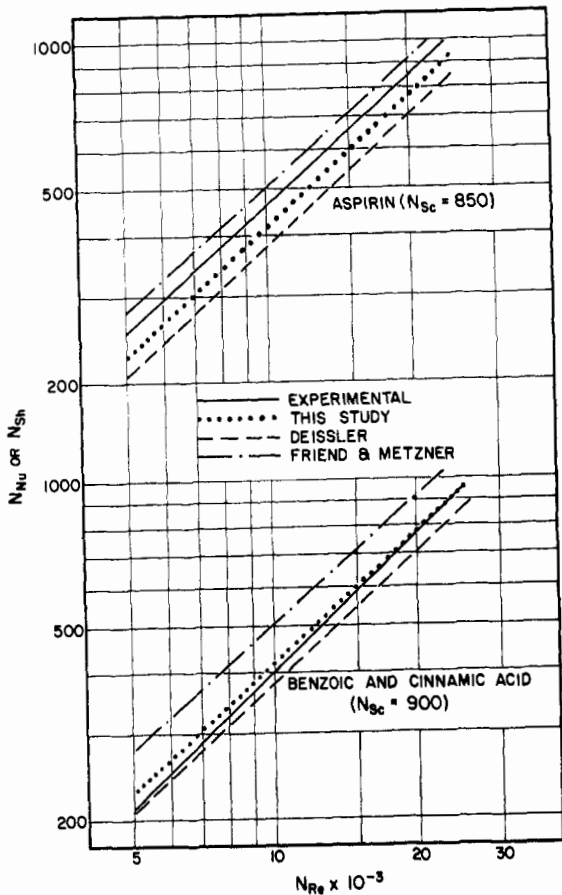
Figure 8. Comparison of Myerink and Friedlander
Data (18) with analytical results

Figure 9. Temperature or concentration distributions for
infinite parallel plates at various N_{Pr} or N_{Sc} for
$N_{Re} = 25,000$

N_{Sc} or N_{Pr} below 1. The flux at a distance from the wall never exceeds the wall flux, in contrast to the results for circular tubes. This is obviously explained by the constant and decreasing transfer area in flat plates and tubes, respectively. The effect of a nonlinear flux distribution changes N_{Sh} on the order of 5 to 6% at N_{Sc} or $N_{Pr} = 1$, and considerably more at lower N_{Pr}. Therefore, its effect should not be neglected, unless N_{Sc} is substantially above 1, if an accurate calculation is desired.

The analytical calculations for flow between flat plates indicate that N_{Nu} values converge to those in tubes at approximately N_{Pr} or $N_{Sc} = 10$. At higher values of N_{Pr} or N_{Sc} the N_{Nu} curves for the two configurations cross and the flat plate values for N_{Sc} or $N_{Pr} = 3000$ are lower than the tube values, but the differences decrease as N_{Re} increases. N_{Nu} or N_{Sh} for the two configurations would be expected to converge rapidly at higher N_{Pr} or N_{Sc} and be identical in the limit $N_{Pr} = N_{Sc} = \infty$. The fairly small deviations exhibited by the calculations from this behavior are attributable to the limitations of the hydraulic radius concept, which is less in error at higher N_{Re}. For example, at $N_{Re} = 10,000$ and $N_{Sc} = 3000$ the calculated N_{Sh} for tubes is approximately 3.5% below the plate value and at $N_{Re} = 100,000$ it is approximately 2.5% lower at the same N_{Sc}. Since the tube calculations are more accurate, the N_{Sh} or N_{Nu} values for plates may be taken equal to those for tubes at N_{Pr} or N_{Sc} above 10. Therefore plate values have not been plotted above this value.

CONCLUSIONS

Small turbulent disturbances in the immediate vicinity of the wall profoundly affect the mass or heat transfer rate, and can therefore be estimated more accurately from heat or 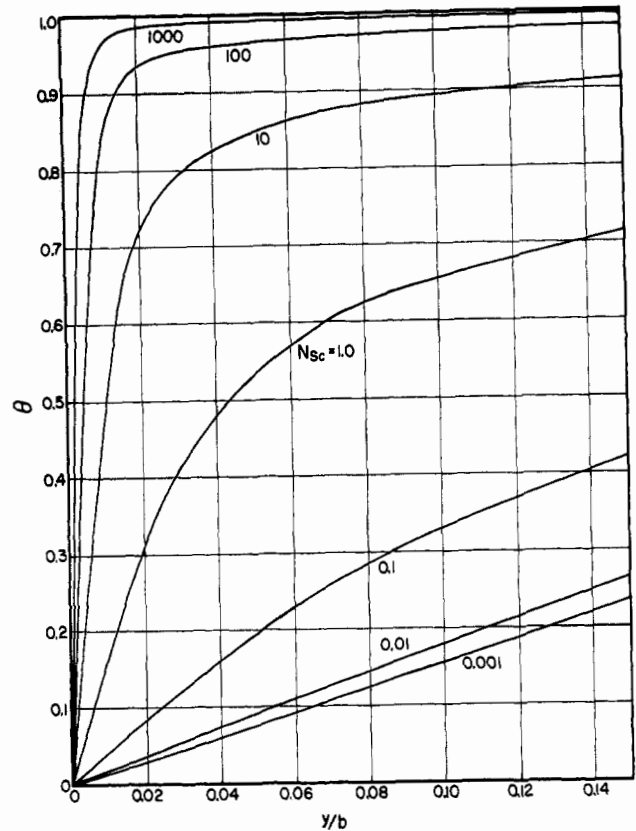mass transfer investigations at high Prandtl or Schmidt numbers than by velocity distribution measurements, which are relatively insensitive to these disturbances.

Heat and mass flux distributions for fully developed parallel flow between infinite parallel plates and in smooth circular tubes differ markedly from one another, whereas the momentum flux is linear in both configurations. For both tubes and plates the heat or mass flux distributions deviate most significantly from linearity at low Peclet numbers, which is the region of interest in studies of liquid metal heat transfer. This in turn results in higher Nusselt numbers for plates than tubes at corresponding Peclet numbers (Figure 5).
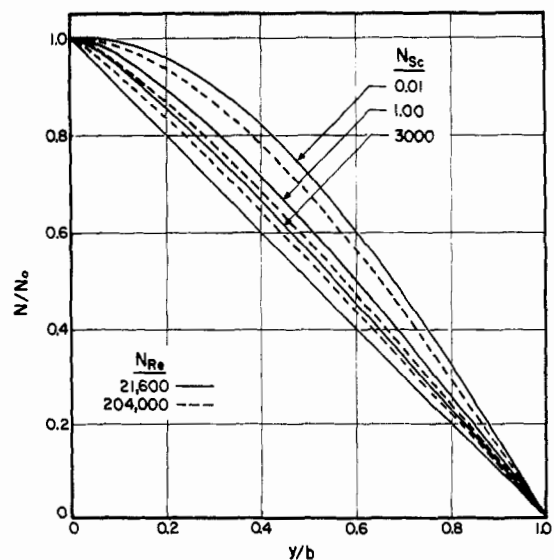

Figure 10. Mass flux distribution for flow
between infinite parallel plates

Further investigation of the velocity distribution between infinite parallel plates seems necessary, since there are significant differences between the existing investigations (20) in the region below $N_{Re} = 30,000$.

The assumption of universally applicable friction factor laws tends to confuse rather than clarify existing inconsistencies in the available experimental heat and mass transfer data. This is particularly detrimental when the objective is to obtain further insight concerning turbulence near solid boundaries, which is markedly influenced by surface irregularities. Future experimental investigations should include friction factor and heat or mass transfer measurements to reduce the uncertainty concerning this effect in a given system.

NOMENCLATURE

b = r_0 for tubes and half channel width for parallel plates, L
C = concentration of solute, m/L^3
D = molecular diffusivity, L^2/t
d = diameter, L
f = friction factor
h = heat transfer coefficient
k = mass transfer coefficient
K = thermal conductivity
N = local mass flux, $m/L^2 t$
q = heat flux, m/t^3
r = radius, L
T = temperature
T = shear stress, m/Lt^2
$\bar{u}$ = time average point velocity in x direction, L/t
U = bulk mean velocity in x direction, L/t
u^+ = dimensionless velocity parameter, $\bar{u}/(\text{T}_0/\rho_0)^{1/2}$
x = distance along axis, L
y = distance from wall, L
y^+ = dimensionless distance parameter, $y(\text{T}_0/\rho_0)^{1/2}/\nu$

Dimensionless Groups

N_{Re} = Reynolds number for tubes $V\rho d/\mu$ for parallel plates $4V\rho b/\mu$
N_{Sc} = Schmidt number, $\mu/\rho D$
N_{Sh} = Sherwood number, kd/D
N_{Nu} = Nusselt number, hd/K
N_{Pr} = Prandtl number, $C_p\mu/K$
N_{Pe} = Peclet number, $N_{Pr}N_{Re}$

Subscripts

b = bulk mean value
c = centerline value
d = mass transfer
e = equivalent
0 = value at wall

Greek Letters

β = dimensionless velocity, $\bar{u}/u_{max}$
ϵ = eddy diffusivity, L^2/t
ϵ_d = eddy diffusivity (mass), L^2/t
ν = kinematic viscosity, L^2/t
ρ = density, m/L^3
μ = viscosity, m/Lt

θ = dimensionless temperature or concentration, $\left(\dfrac{C - C_0}{C_c - C_0}\right)$, $\left(\dfrac{T - T_0}{T_c - T_0}\right)$

LITERATURE CITED

(1) Cairns, R.C., Roper, G.H., Chem. Eng. Sci. 3, 97 (1954); 4, 221 (1955).
(2) Chilton, T.H., Colburn, A.P., Ind. Eng. Chem. 26, 1183 (1934).
(3) Deissler, R.G., Natl. Advisory Comm. Aeronaut., Tech. Note 2138 (1950).
(4) Ibid., Research Memo. E52F05 (1952).
(5) Ibid., Rept. 1210 (1955).
(6) Eckert, E.R.G., Drake, R.M., "Heat and Mass Transfer," McGraw-Hill, New York, 1959.
(7) Eckert, E.R.G., Hartnett, J.P., Trans. Soc. Mech. Engrs. 79, 247 (1957).
(8) Eckert, E.R.G., Schneider, P.J., J. Aeronaut. Sci. 23, 384 (1956).
(9) Fage, A., Townend, H.C.H., Proc. Roy. Soc. (London) 135A, 656 (1932).
(10) Friend, W.L., Metzner, A.B., A.I.Ch.E. Journal 4, 393 (1958).
(11) Hinze, J.O., "Turbulence," p. 551, McGraw-Hill, New York, 1959.
(12) Isakoff, S.E., Drew, T.B., "Proceedings of General Discussion on Heat Transfer," Inst. Mech. Engrs., London, and Am. Soc. Mech. Engrs., p. 405, 1951.
(13) Lin, C.S., Moulton, R.W., Putnam, G.L., Ind. Eng. Chem. 45, 636 (1953).
(14) Linton, W.H., Sherwood, T.K., Chem. Eng. Progr. 46, 258 (1950).
(15) Lyon, R.N., Ibid., 47, 75 (1951); Oak Ridge Natl. Lab. Rept. ORNL 361 (1949).
(16) Martinelli, R.C., Trans. Am. Soc. Mech. Engrs. 69, 947–59 (1947).
(17) Merk, H.J., Appl. Sci. Research A8, 73 (1959); A8, 100 (1958); A8, 237, 261 (1959).
(18) Meyerink, E.S.C., Friedlander, S.K., "Diffusion Controlled Reactions in Fully Developed Pipe Flow," Report on Natl. Sci. Found. Grant G5079 (May 1960).
(19) Mickley, H.S., Ross, R.C., Squyers, A.L., Stewart, W.E., Natl. Advisory Comm. Aeronaut., Tech. Note 3208 (1954).
(20) Opfell, J.B., Sage, B.H., "Advances in Chemical Engineering," T.B. Drew, J.W. Hoopes, eds., vol. 1, Academic Press, New York, 1956.
(21) Page, F., Schlinger, W.G., Breaux, D.K., Sage, B.H., Ind. Eng. Chem. 44, 424 (1952).
(22) Poppendiek, H.F., Natl. Aeronaut Space Admin., Memo 2-5-59W (1959).
(23) Reichardt, H., Natl. Advisory Comm. Aeronaut., Tech. Note 1408 (1957).
(24) Seban, R.A., Shimazaki, Trans. Am. Inst. Mech. Engrs. 73, 803 (1951).
(25) Severson, E.E., Madden, A.J., Piret, E.L., A.I.Ch.E. Journal 5, 413 (1959).
(26) Sherwood, R.K., Trans. Inst. Chem. Engrs. 36, 817 (1940).
(27) Smith, J.W., J. Aeronaut. Sci. 21, 154 (1954).
(28) Spalding, D.B., Proc. Roy. Soc. London A221, 78 (1953).
(29) Van Driest, E.R., J. Aeronaut. Sci. 23, 1007 (1956).
(30) Westaemper, L.E., White, R.R., A.I.Ch.E. Journal 3, 69 (1956).